of parity conservation in this decay. We merely note here that, at the moment, no direct evidence is available for or against parity conservation in high-energy electromagnetic interactions of strange particles.

Our main interest in this paper has been to devise a means of determination of the $\Sigma^0$ lifetime, $\tau(\Sigma^0)$, which remains the only unknown elementary particle lifetime. We conclude that the study of approximately forward $\Lambda^0 \rightarrow \Sigma^0$ conversion in a high-$Z$ nuclear Coulomb field may well provide a feasible experimental procedure of finding $\tau(\Sigma^0)$.

We also suggest that the $\Sigma^0$ lifetime may be determined from an analysis of $\Sigma^{\pm} \rightarrow \Lambda^0$ strangeness-conserving leptonic decays if these decays are subject to a principle of "minimal weak coupling" and the associated assumption of a conserved baryon-meson polar-vector current, and if the effective axial vector coupling is not dominant. We emphasize that the advent of machines of high beam intensity should eventually permit a fairly detailed study of $\Sigma^{\pm} \rightarrow \Lambda^0 + e^{\pm} + \nu$ and, in view of the expected "anomalous" features of these decays, point out that the corresponding decay rates and electron momentum spectra will surely provide important weak-interaction data even if they should prove incapable of yielding the value[26] of $\tau(\Sigma^0)$.

[26] For the sake of completeness we mention that one can write the weak-electromagnetic branching ratio

$$B \equiv \text{Rate}[\Sigma^0 \rightarrow p + \pi^-]/\text{Rate}[\Sigma^0 \rightarrow \Lambda^0 + \gamma]$$
$$= \text{Rate}[\Sigma^+ \rightarrow p + \pi^0]/\text{Rate}[\Sigma^0 \rightarrow \Lambda^0 + \gamma],$$

the second equality following upon use of the $\Delta T = \frac{1}{2}$ rule. Thus any future measurement of $B$ together with already available empirical information about $\text{Rate}[\Sigma^+ \rightarrow p + \pi^0] = 6 \times 10^9$ sec$^{-1}$ is sufficient to determine $\text{Rate}[\Sigma^0 \rightarrow \Lambda^0 + \gamma] = 1/\tau(\Sigma^0)$. This weak-electromagnetic branching ratio method will be the least impractical method for determination of $\tau(\Sigma^0)$ if $\tau(\Sigma^0)$ is appreciably greater than the $10^{-18}$–$10^{-20}$ sec now anticipated [Eq. (11d)] since in this case the methods discussed in Secs. III and IV will become prohibitively difficult.

PHYSICAL REVIEW VOLUME 125, NUMBER 5 MARCH 1, 1962

# Precision Measurement of the $\mu^+$ Lifetime*†

RICHARD A. LUNDY‡
*Enrico Fermi Institute for Nuclear Studies, The University of Chicago, Chicago, Illinois*

(Received September 28, 1961)

A new precision measurement of the mean lifetime of the positive muon, $\tau(\mu^+)$, is described. On the basis of 12 internally consistent, independent determinations performed under a variety of experimental conditions we obtain $\tau(\mu^+) = (2.203 \pm 0.004)$ $\mu$sec. These determinations were performed by means of an improved version of Swanson's "digitron"—a digital electronic time interval measuring device—embodying a continuous wave (CW) oscillator and several protective features. The available experimental conditions, in particular concerning the percentage of background events, were greatly superior to those available in earlier experiments here and elsewhere. Particular attention was paid to sources of systematic error, such as time dependence of background events and rate dependence of the over-all measuring process. All sources of background have been localized, their effects quantitatively exhibited and, in general, suppressed electronically during actual lifetime determinations.

The prediction of the conserved vector-current theory, using $ft(O^{14}) = (3069 \pm 13)$ sec and $m_\mu = 206.76 m_e$, is (including radiative corrections) $\tau(\mu^+) = 2.298 \pm 0.05$ $\mu$sec, and thus in disagreement with the experimental value reported here. This discrepancy is even greater than with the somewhat higher values obtained for $\tau(\mu^+)$ by other workers; these values are briefly reviewed.

A full discussion of the logical operation of the digitron, and of time-interval measuring devices in general, is presented. In Appendix I (by R. Winston) a general formalism is given which establishes the connection between arbitrary interval distributions presented at the input of such devices and their corresponding output interval distributions.

## I. INTRODUCTION

A PRECISION measurement of the mean lifetime, $\tau(\mu^+)$, of muons is of great theoretical interest for several rather well-known reasons. This lifetime is essentially given by the rate for the decay process

$$\mu^+ \rightarrow e^+ + \nu + \bar{\nu}, \qquad (1)$$

in which *only* weakly interacting leptons (as opposed, say, to the baryons in ordinary beta decay) participate. Hence one can extract from $\tau(\mu^+)$ valuable information concerning the absolute magnitudes of the "true" coupling constants, i.e., their magnitudes with the "renormalizing" effect of strong interactions switched off. All present-day evidence[1] concerning process (1) is compatible with the assumption that it is described by the $(V-A)$ interaction, i.e., that only two types of coupling $(V,A)$ intervene in the relevant Fermi interaction and that the absolute magnitudes of the corresponding coupling constants are equal: $|C_V| = |C_A| = G$. Thus, there appears to be only one fundamental coupling constant, $G$, for weak interactions and its measure is given by $\tau(\mu^+)$.

* Research supported by a joint program of the Office of Naval Research and the U. S. Atomic Energy Commission.

† Based on a thesis submitted to the Faculty of the Department of Physics, the University of Chicago, in partial fulfillment of the requirements for the Ph.D. degree.

‡ National Science Foundation Fellow, 1958–1959, 1959–1960.

[1] V. L. Telegdi, *Proceedings of the 1960 Annual International Conference on High-Energy Physics at Rochester* (Interscience Publishers, Inc., New York, 1960), p. 713.

This constant $G$ is the more fundamental that the hypothesis of a universal Fermi interaction—namely that other weak interactions such as beta decay and muon capture should also be of the form $(V-A)$—is to a large extent supported, and nowhere contradicted, by the available experiments.[1] In principle, however, the values of both $C_V$ and $C_A$ could differ, in the processes just mentioned, from $G$ because of the anticipated (but uncalculable) effects of strong virtual processes. Feynman and Gell-Mann,[2] by analogy with electromagnetism and reviving an idea of Gershtein and Zel'dovich,[3] have proposed that while $C_A$ (say, in beta decay) could depart from $G$ in virtue of such processes by an essentially unknown factor, $C_V$ would maintain its value, $G$, in *all* processes. $C_V$, the "charge" of the weak vector interaction, would have, like $e$, the charge of the electromagnetic (vector) interaction, the same universal value $G$ independent of the type of particles carrying it.

Thus, a precision measurement of $\tau(\mu^+)$, combined with a precision measurement of $C_V$ (from the $ft$ value of a pure $V$ nuclear beta transition), could serve, as emphasized by Feynman and Gell-Mann, as a check of their conserved vector-current hypothesis.

Accepting the $ft$ value[4] $(3069\pm13)$ sec for the pure $V$ (i.e., $O^+ \rightarrow O^+$) transition $O^{14} \rightarrow N^{14*}$, one predicts

$$\tau(\mu^+)=(2.250\pm0.01)\ \mu\text{sec}, \qquad (2)$$

neglecting radiative corrections to both muon and beta decay. The latter, as computed by Berman[5] and by Kinoshita and Sirlin,[6] raise the predicted value to

$$\tau(\mu^+)=(2.298\pm0.05)\ \mu\text{sec}. \qquad (3)$$

Several recent determinations of $\tau(\mu^+)$,[7–10] while scattered in tolerable agreement with each other about a mean value of $(2.214\pm0.004)$ $\mu$sec, appear to be in significant disagreement $(4\pm1\ \%)$ with the more reliable theoretical prediction, i.e., Eq. (3).[10a]

Using a different approach to the concept of "universality," i.e., abandoning the hypothesis that the bare coupling constants are the same before turning on the electromagnetic interaction, Durand, Landowitz, and Marr[11] have obtained radiative corrections which have the *same* sign for muon and beta decay. Their prediction is hence essentially the value (2), and therefore still in disagreement (by $1.8\pm0.5\ \%$) with experiment.

While presently available muon intensities should enable one, from the point of view of statistics alone, to measure $\tau(\mu^+)$ to an accuracy far exceeding the uncertainties attached by theoreticians to predictions such as (3) (viz., $\pm1.0\%$) and greater than the currently quoted accuracies of the relevant $ft$ values (0.4%), severe limitations are set to such a measurement by numerous sources of systematic errors.

The purpose of this paper is to present not only a new and very precise determination of $\tau(\mu^+)$ based on 12 independent measurements done in a variety of experimental conditions but also an attempt at a particularly careful discussion of systematic errors.[12] These measurements, as compared to earlier ones, were performed under greatly improved conditions (in particular, of background). The electronic equipment used, aside from providing a highly linear, absolute time scale, was so designed as to minimize the effects of the sources of systematic errors known to us.

## II. EXPERIMENTAL METHOD

### A. Beam Layout and Counting Arrangement

Positive pions at rest decay via $\pi^+ \rightarrow \mu^+ + \nu$ with a lifetime of about 25 m$\mu$sec. This is much shorter than the muon lifetime of about 2 $\mu$sec, and hence a stopped $\pi^+$ beam may constitute a convenient source of unpolarized $\mu^+$'s. We utilized this fact in the experimental arrangement indicated in Fig. 1.[13]

A $\pi^+$ beam of 150 Mev/$c$ momentum from the Chicago synchrocyclotron was obtained in the usual fashion, using however, a vibrating Be target rather than a stationary one.[14] This target provides beams with a duty factor $D=$(instantaneous rate/average

[2] R. P. Feynman and M. Gell-Mann, Phys. Rev. **109**, 193 (1958). For a review of the recent status of this theory, see R. P. Feynman, *Proceedings of the 1960 Annual International Conference on High-Energy Physics at Rochester* (Interscience Publishers, Inc., New York, 1960), p. 501.

[3] S. S. Gershtein and Ya. B. Zel'dovich, J. Exptl. Theoret. Phys. U.S.S.R. **29**, 698 (1953).

[4] R. K. Bardin, C. A. Barnes, W. A. Fowler, and P. A. Seeger, Phys. Rev. Letters **5**, 323 (1960).

[5] S. M. Berman, Phys. Rev. **112**, 267 (1958).

[6] T. Konoshita and A. Sirlin, Phys. Rev. **113**, 1652 (1959).

[7] J. Fischer, B. Leontic, A. Lundby, R. Meunier, and J. P. Stroot, Phys. Rev. Letters **3**, 349 (1959).

[8] R. A. Reiter, T. A. Romanowski, R. B. Sutton, and B. G. Chidley, Phys. Rev. Letters **5**, 22 (1960).

[9] Quoted in references 1 and 8.

[10] A. Astbury, P. M. Hattersly, M. Hussain, A. Kemp, and H. Muirhead, *Proceedings of the 1960 Annual International Conference on High-Energy Physics at Rochester* (Interscience Publishers, Inc., New York, 1960), p. 542.

[10a] *Note added in proof.* R. J. Blin-Stoyle and J. Le Tourneux [Phys. Rev. **123**, 627 (1961)] have calculated the effect of a *charge-dependent* internucleon potential on the $O^{14}$ $(0^+, T=1) \rightarrow N^{14*}$ $(0^+, T=1^+)$ matrix element. They find $M_F^2=2(1-\delta)$, where $\delta=1$ or 2% for reasonable strength and form of such a potential. This reduction might be of the right order of magnitude to resolve this disagreement while maintaining the concept of a conserved universal $V$ coupling.

[11] L. Durand, III, L. F. Landovitz, and R. B. Marr, Phys. Rev. Letters **4**, 620 (1960).

[12] A preliminary version of this determination was performed here in October, 1959 by J. Lathrop, R. Lundy, R. Swanson, V. L. Telegdi, D. D. Yovanovitch, and R. Winston, with the result $\tau(\mu^+)=(2.208\pm0.005)$ $\mu$sec. This constituted the material for reference 9.

[13] This arrangement is very similar to one previously used here for the same purpose, and described in R. A. Swanson, R. A. Lundy, V. L. Telegdi, and D. D. Yovanovitch, Phys. Rev. Letters **2**, 430 (1959). The value for $\tau(\mu^+)$ reported in that reference is now believed to have been the result of systematic errors that went undetected. Unfortunately, the "digitron" then used was disposed of before this situation became apparent, so that a systematic investigation *a posteriori* became impossible.

[14] J. Rosen, Bull. Am. Phys. Soc. **6**, 9 (1961).

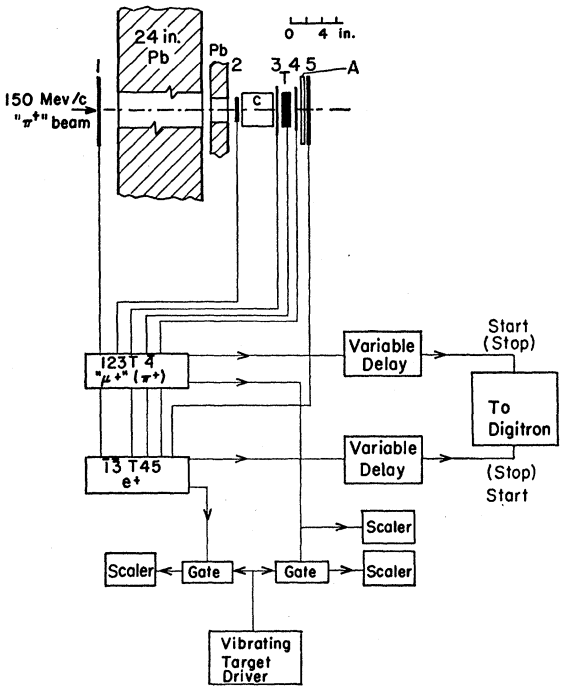


FIG. 1. Experimental arrangement for the measurement of $\tau(\mu^+)$. 1, 2, 3, T, 4, and 5 are plastic scintillators, viz., $1=8\times8\times\frac{3}{8}$ in., $2=3\times3\times\frac{1}{4}$ in., $3=5\times5\times\frac{1}{8}$ in., $T=4\times4\times1$ in., $4=5\times5\times\frac{1}{4}$ in., $5=8\times8\times\frac{3}{8}$ in. $C=15$ g/cm² graphite moderator, $A=1$g/cm² $(CH_2)_n$ moderator.

rate) = 5 as compared to $D=50$ in the case with stationary targets. This reduction in instantaneous rate is very beneficial: accidental backgrounds are proportionately reduced, and dead-time and pulse pile-up are no longer serious problems.

$\pi^+$'s pass through a 4-in. diam hole in a 2-ft thick Pb wall and are further collimated by a 3-in. diam hole in a Pb shield. The moderator (15 g/cm² of graphite) brings them to rest in a 4-in. square, 1-in. thick plastic scintillator $T$. This is chosen sufficiently thick to contain the range-spread of the $\pi^+$ beam used. A stopping particle, i.e., a $\pi^+$, generates a coincidence $(123\,\bar{4})$, somewhat incorrectly called the "$\mu^+$ telescope" output. The beam also contains $\mu^+$ (5%) and a negligible number of $e^+$, having longer ranges than $\pi^+$'s, and these trip the anticoincidence counter $\bar{4}$.

The $\pi^+$'s stopped in $T$ decay isotropically into $\mu^+$'s of 0.2-g/cm² range. This range is so short that only a very few $\mu^+$'s escape from $T$. $\mu^+$'s stopped in $T$ decay into $e^+$'s and the $e^+$'s are detected by the "$e^+$ telescope", consisting of the coincidence combination $(\bar{1}\bar{3}T45)$.

Because of the anisotropy of $\mu^+$ decay it is important that the $\mu^+$'s do not precess in the stray magnetic field of the cyclotron. We guard against this by beginning with unpolarized $\mu^+$'s, reducing the magnetic field in the vicinity of $T$ to less than 0.1 gauss with bucking coils, and using a polystyrene scintillator which partially depolarizes $\mu^+$'s.

The counters described above consist of plastic scintillators coupled by UVT Lucite light pipes to 6810 A photomultipliers. The coincidence circuits employed are of Garwin design[15] and give resolutions of about 20 mμsec. The delay lines indicated in Fig. 1 are HH-2000 cable.

### B. Principle of Lifetime Measurement

If a pulse from the $\mu^+$ telescope is taken as zero time, the time distribution of $e^+$ telescope output pulses will be

$$N(t)=\frac{\exp[-t/\tau(\pi^+)]-\exp[-t/\tau(\mu^+)]}{\tau(\pi^+)-\tau(\mu^+)}+B(t), \quad (4)$$

where $\tau(\pi^+)$ is the pion lifetime and $B(t)$ represents the background as defined below. By retaining only that part with $t\geq\tau(\pi^+)$ [say $t=10\tau(\pi^+)$] the effect of the $\pi^+$ lifetime may be neglected, and we can take

$$N(t)=\exp[-t/\tau(\mu^+)]+B(t), \quad t>10\tau(\pi^+). \quad (5)$$

The equipment employed in the experiment ("digitron") does not yield $N(t)$ directly, but a slightly different function $O(t)$.[16] This distortion results from the fact that digitron (as well as other conventional time-to-pulse-height converters) measures time elapsed between a given start pulse and the *first* stop pulse to come along. If a start pulse is followed, within the measuring interval $T$, by two or more stop pulses, then the first one of these will be recorded with unit efficiency and all the others with zero efficiency. The exact form of the output interval distribution $O(t)$ resulting from a given input interval distribution $I(t)$ is calculated in Appendix I. If the probability of such multi-stop events is known, it becomes possible to calculate $I(t)$ from the recorded $O(t)$. These computed corrections may, however, be quite large and they require accurate measurements of the instantaneous stop rates. A more direct approach consists in eliminating all events in which more than one stop occurs within $T$. This is achieved by the "interference remover" circuits to be described below.

### C. Sources of Background and their Removal

The function $B(t)$ representing the probability distribution of background events might be thought to be well approximated by a constant. This is however *not* the case in general. Consider the following type of event: A $\mu^+$ is produced in the target counter and digitron is started; before this $\mu^+$ decays, a second $\mu^+$ is produced and decays into the $e^+$ telescope, producing

[15] R. L. Garwin, Rev. Sci. Instr. 24, 618 (1953).

[16] This important fact was first recognized by R. A. Swanson [Phys. Rev. 112, 580 (1958)], who computed the output of a time converter presented at its input with a single source and an uncorrelated background. Swanson's model does *not* apply under experimental conditions such as ours, where multi-stop events—rather than uncorrelated electrons—are the dominant source of background. (See Appendix I for definitions.)

a stop pulse. This sort of event leads to a background which increases as one goes away from $t=0$. An expression for its functional dependence on $t$ is deduced in Appendix I (case Ic). This so-called "growth background" may be eliminated by rejecting decays whenever more than one start pulse occurs during the measuring interval $T$. This function is performed electronically by the "interference removers" (see subsection II-D-5).

An additional source of time-dependent background, (example d of Appendix I) consists of the following: A $\mu^+$ is produced in the target during the dead-time $T_d$ of digitron and is undetected. Subsequently a second $\mu^+$ starts digitron and an $e^+$ from the first $\mu^+$ makes a stop pulse. This type of background is *not* eliminated by interference removers. The effect is observable (see subsection III-B) but is negligible at the rates used in our experiments.

If the two telescopes counted only stopping $\pi^+$'s and only $e^+$'s from a detected $\pi-\mu-e$ decay chain in the target, the above considerations would eliminate all background events and make $B(t)=0$. This, however, is not the case, mainly because there is always a small accidental coincidence rate present in the $e^+$ telescope, typically $\sim 3\%$ in most of our runs. These accidental counts, referred to as "uncorrelated" or "parentless" $e^+$'s, inasmuch as they are most likely $e^+$'s produced from $\mu^+$'s stopping in parts of the apparatus other than the target, lead to background in the following way: A $\mu^+$ starts the digitron but its decay $e^+$ misses the $e^+$ telescope. An uncorrelated $e^+$ stops the digitron; this satisfies the condition that there be only one start and only one stop pulse in the interval $T$, and so these events are not eliminated by the interference removers. Such events give rise to a background $B_0$ which is constant in time. Defining $\lambda$, the ratio of true event rate $N(0)$ to the background rate $B_0$ at zero time, we have

$$\lambda \equiv N(0)/B_0 = 1/[fR\tau(\mu^+)(1-\omega)], \qquad (6)$$

where $\omega$ is the fractional solid angle subtended by the $e^+$ telescope, $f$ is the ratio of uncorrelated $e^+$'s to true

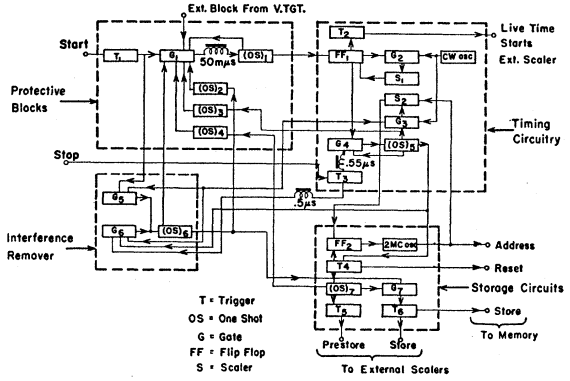


FIG. 2. Block diagram of digitron.

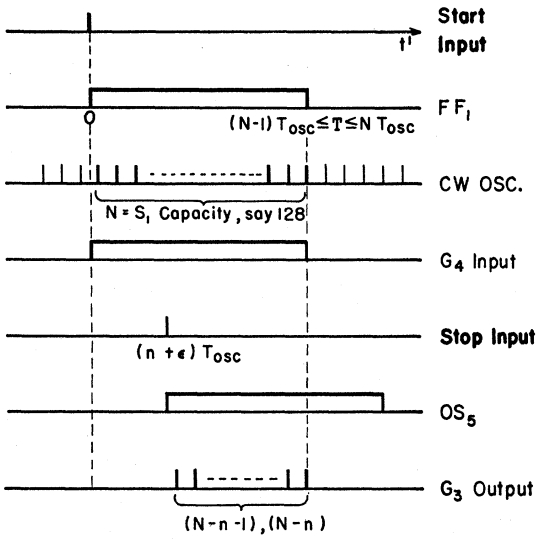


FIG. 3. Timing diagram of digitron (abbreviations $FF_1$, $G_4$, etc. refer to Fig. 2).

decay $e^+$'s at zero time, $R$ is the $\mu^+$ rate, and $\tau(\mu^+)$ the muon mean lifetime.

Up until now we have considered the $\mu^+$-telescope output as a start pulse and the $e^+$-telescope output as the stop pulse, i.e., the *natural* time order in which these pulses do occur. One can delay the $\mu^+$ pulses by more than $T$ and operate the digitron with $e^+$ starts and $\mu^+$ stops; this we call the "*inverted*" order. There is no logical difference between the two orders, and both give the same expression for $\lambda$, but the inverted order (where $e^+$'s start) reduces dead-time losses. In most of our runs the time scale of the digitron was so adjusted that about $10\tau(\mu^+)$ was available for determining $N(t)$ and about $4\tau(\mu^+)$ before zero time could be used for a measurement of $B_0$.

## D. Operating Logic of "Digitron"

### 1. General Considerations

The "digitron" described here is an improved version of an instrument already described by Swanson.[17] As in that instrument, the time interval between two pulses is determined by counting the number of oscillator pulses contained therein and storing this digital information in a magnetic core memory.

The most significant conceptual modification of our digitron with respect to Swanson's instrument consists in replacing the pulsed timing oscillator of reference 17 with a continuously running (CW) crystal-controlled oscillator (Garwin,[18] as well as Sutton *et al.*,[8] have independently constructed instruments embodying CW crystal oscillators, but use an internal logic different from ours). With this feature, stability and linearity

[17] R. A. Swanson, Rev. Sci. Instr. **31**, 149 (1960).
[18] R. L. Garwin (private communication).

are much improved. As opposed to Swanson's vacuum-tube instrument,[17] our digitron is constructed almost entirely from a few basic circuits utilizing 2N501 transistors and fast diodes. The use of transistors facilitates the dc coupling of many stages, thus reducing the rate dependence of the over-all operation.

A block diagram of the digitron is given in Fig. 2, and the time relationships of various pulses referred to below are illustrated in Fig. 3.

### 2. *Protective Blocking Circuits*

The time required to analyze a pair of pulses, i.e., the dead-time $T_d$ of the digitron, is approximately 500 $\mu$sec. During this time the input must be blocked to prevent subsequent pulses from interfering with the analysis and data storage. This is accomplished by passing the start pulses from the trigger $T_1$ through the normally open gate $G_1$ which can be closed by one-shots $(OS)_1$, $(OS)_2$, $(OS)_3$, $(OS)_4$, $(OS)_6$, or an external signal. These one-shots are triggered by pulses derived from other parts of the instrument. The output pulse length and relative timing is so adjusted that each one shot has ample recovery time.

### 3. *Timing Circuitry*

After passing through the block circuits just described, a start pulse sets a flip-flop $FF_1$ which opens the normally closed gate $G_2$. Pulses from the CW oscillator are then transmitted and fill the scaler $S_1$ (of capacity $N$, say 128) until an output from it resets $FF_1$ closing $G_2$. In this manner a measuring interval $T$ is defined: its leading edge by the start pulse and its trailing edge by the last pulse of the oscillator train. The length of the interval will vary from $N$ to $N-1$ oscillator periods, $T_{osc}$, depending upon the initial random phase between the start pulse and the oscillator. $FF_1$ also opens a normally closed gate $G_4$ and allows stop pulses from a trigger $T_3$ to operate one-shot $(OS)_5$ whose output pulse length is adjusted to be greater than the measuring interval $T$.

The outputs from $(OS)_5$, $FF_1$, and the oscillator are applied to the normally closed triple gate $G_3$. The output of $G_3$ consists of those oscillator pulses occurring during the overlap of $(OS)_5$ and $FF_1$. The stop pulse also has a random phase relation to the oscillator and so the output of $G_3$ will consist of a pulse train having a first pulse of varying amplitude but all other pulses (including the final one) of a well-defined shape. This output of $G_3$ is fed into scaler $S_2$ which has the same capacity as $S_1$. $S_2$ will thus be filled to some number, representing approximately the complement of the time interval between start and stop pulses. For a given fixed separation, $(n+\epsilon)T_{osc}$, between start and stop pulses the number stored in $S_2$ will be $(N-n)$ or $(N-n-1)$ because of the random phase of the start pulse relative to the oscillator. For this reason in general two channels (of the multi-channel analyzer into which data are ultimately stored) will be populated; the ratio of their populations allows one to locate the stop pulse in time to a fraction of a channel width with an accuracy determined primarily by the statistics of the populations of the two adjacent channels.

### 4. *Storage Circuits*

The magnetic core memory used is a portion of a commercial multi-channel pulse-height analyzer.[19] Three pulses are required to operate such a memory from an external source: (1) a "reset" pulse which sets the address and the arithmetic scalers to zero; (2) an "address" pulse which advances the address scaler to the appropriate channel, and (3) a "store" pulse which causes the arithmetic circuits to add one count to the channel selected by the address pulse.

The required "reset" pulse is generated by a stop pulse and is timed to occur after the timing circuits have finished their analysis. $T_4$, the reset trigger in the storage circuit also sets a flip-flop, $FF_2$, which starts a gated 2-Mc/sec oscillator. Pulses from the oscillator are fed into scaler $S_2$ and cause it to advance from the count $(N-n)$ or $(N-n-1)$ deposited by the timing circuits to its full capacity. An output from $S_2$ then resets $FF_2$, stopping the 2-Mc/sec oscillator. This train of 2-Mc/sec oscillator pulses advances the memory address-scaler thus selecting the appropriate address in the memory which represents the time interval between start and stop. When addressing is completed, a pulse from $(OS)_7$ passes through a normally open gate $G_7$ and triggers $T_6$ which initiates the memory storage cycle.

### 5. "*Interference Removers*"

These circuits as explained above (subsection II-C) are useful in two ways: (a) in reducing the percentage of background events; (b) in eliminating the possible difference between the input interval distribution $I(t)$ presented to the digitron and its corresponding output distribution, $O(t)$. (See Appendix I.)

$G_5$ is a double "and" gate which makes an output if a second start pulse arrives during the interval $T$. $G_6$ is a triple "and" gate which makes an output if a second stop pulse arrives during the interval $T$. An output from either gate triggers $(OS)_6$ which by closing gate $G_7$ prevents any store pulse from reaching the memory.

### 6. *Miscellaneous Features*

The dead time $T_d$ of this instrument is by necessity fairly large and a knowledge of it is essential. $T_d$ can be measured by counting the output of $T_2$ (referred to as "live time starts") and comparing it to the number of

[19] Radiation Instruments Development Laboratory, Chicago, Illinois.

TABLE I. Experimental results.[a]

| Run | $R$ $\times 10^{-3}$ | Total counts $\times 10^{-5}$ | $\tau_\mu$($\mu$sec) | $B_{\text{fit}}$ | $B_{\text{exp}}$ | $B_{\text{calc}}$ | $\lambda \times 10^{-3}$ | $K \times 10^3$ | $\chi^2/\langle\chi^2\rangle$ |
|---|---|---|---|---|---|---|---|---|---|
| 1($n$) | 4.3 | 10 | 2.208±0.006 | 158 ±40 | ··· | ··· | 0.33±0.08 | 2.0 ±2.4 | 1.04±0.18 |
| 2($n$) | 3.0 | 10 | 2.209±0.004 | 89 ±18 | ··· | ··· | 0.59±0.12 | −0.6 ±1.6 | 0.89±0.07 |
| 3($i$) | 0.5 | 10 | 2.198±0.002 | 11.6± 3.0 | 11.0±0.5 | ··· | 9.9 ±2.5 | 0.8 ±0.7 | 0.96±0.17 |
| 4($i$) | 2.1 | 10 | 2.201±0.003 | 13.6± 3.0 | 13.6±0.5 | ··· | 5.5 ±1.3 | −0.2 ±0.9 | 0.94±0.17 |
| 5($i$) | 1.1 | 3 | 2.198±0.004 | 2.7± 1.0 | 2.6±0.4 | 3.0 | 20 ±7 | 0.7 ±0.7 | 1.42±0.24 |
| 6($i$) | 1.6 | 3 | 2.209±0.004 | 4.8± 1.0 | 4.6±0.5 | 4.4 | 12 ±2.4 | −0.5 ±1.1 | 1.51±0.26 |
| 7($i$) | 3.5 | 5 | 2.199±0.003 | 10.7± 0.7 | 9.5±1.0 | 9.8 | 5.6 ±0.36 | −1.3 ±0.7 | 1.40±0.21 |
| 8($i$) | 5.4 | 5 | 2.204±0.003 | 13.5± 0.8 | 12.9±1.0 | 15.0 | 4.3 ±0.3 | 0.45±0.78 | 1.15±0.17 |
| 9($i$) | 8.8 | 5 | 2.210±0.003 | 25.9± 1.0 | 27.0±1.0 | 26.0 | 2.3 ±0.1 | −0.30±0.78 | 1.08±0.15 |
| 10($n$) | 1.1 | 3 | 2.204±0.005 | 1.1± 0.3 | ··· | 1.4 | 23 ±6.5 | −0.90±1.10 | 0.80±0.12 |
| 11($n$) | 3.2 | 5 | 2.205±0.003 | 9.5± 0.6 | ··· | 10.0 | 6.4 ±0.4 | 1.4 ±1.0 | 1.04±0.15 |
| 12($n$) | 5.1 | 5 | 2.206±0.003 | 14.4± 0.8 | ··· | 17.0 | 4.5 ±0.3 | −2.1 ±0.7 | 1.14±0.16 |

[a] $n$ =normal order; $i$ =inverted order; $R=\mu^+$ rate; $B_{\text{fit}}$ =background found with least-squares fit; $B_{\text{exp}}$ =background found from $t<0$ data; $B_{\text{calc}}$ =background found with relation (6); $\lambda = N(0)/B_0$; $K$: see Sec. III-D.

start pulses presented at the input. If $\bar{T}$ is the mean time between start pulses, then

$$(\text{outputs of } T_2)/(\text{start inputs}) = \bar{T}/(\bar{T}+T_d). \quad (7)$$

It is also useful to know the number of start pulses which were followed by stop pulses within the measuring interval $T$. When the interference removers are operative, some events are suppressed; thus the number of events in the memory cannot be used for this purpose. An output taken ahead of the gate $G_7$ ("prestore") can be counted and used to determine the total number of events.

By counting both the number of store pulses (output of $T_6$) and the prestore pulses, the number of cancelled events can be determined. This number and the average start input rate $r$ (i.e., the average $\mu^+$ stop rate if the digitron is operated in the natural order) can be combined to yield $R$, the instantaneous rate; clearly $R/r=D$ is the duty factor, and we have

$$\text{cancellations/event} = RT = DrT, \quad (RT \ll 1). \quad (8)$$

The approximation in the above expression consists in neglecting the interference cancellations due to the $e^+$ rate in the "remover" on the stop side.

A check on the reliability of the memory is made by counting the number of store pulses and comparing it to the total contents of the memory.

## III. CALIBRATIONS AND RESULTS

### A. Digitron Calibrations

The earliest measurements (runs 1 and 2 in Table I) in the series described below were made with a digitron embodying a pulsed oscillator operating at about 10 Mc/sec, while the remaining runs used a digitron containing a CW crystal oscillator. In order to evaluate the $\mu^+$ lifetime, one must have an accurate knowledge of the time channel width and the instrument's linearity. This can be obtained in several independent ways:

*1. Statistical method.* This method as described by Weber *et al.*[20] consists of starting digitron with random pulses (derived from a radioactive source) and stopping it with a pulse generator whose period $T_c$ is known and is less than $T$, the range of the digitron. The number of counts accumulated per channel, $n_i$, can be used to evaluate the channel width $\delta_i$, by the relation

$$\delta_i = (n_i/\textstyle\sum n_i)T_c. \quad (9)$$

The pulse generator is usually a crystal oscillator so that $T_c$ is known to 0.01% or better. The error on $\delta_i$ is then just the statistical error of $n_i=\sqrt{n_i}$. A typical measurement accumulated about $10^6$ counts/channel leading to an accuracy in $\delta_i$ of about 0.1%. These measurements were carried out at start rates $R$ ranging from 10/sec to $10^4$/sec. No variations in $\delta_i$ with rate were observed in this range.

*2. Pulse pair method.* This method consists of generating start and stop pulses of known time separations using a calibrated delay line. The accuracy which it can yield is typically about 0.5%. We have used this method to verify the resolution function described in Sec. II-D-3. (A knowledge of this resolution function is necessary for one of the data-analysis methods employed, see Appendix II.)

*3. Direct measurement of oscillator frequency.* With instruments involving pulsed oscillators a direct frequency measurement is limited in practice by the relation $\Delta\omega\Delta t \geq 1$, where $\Delta t$ is the time during which the oscillator is pulsed on. For our applications $\Delta t$ was about $10^{-5}$ sec so $\Delta\omega \simeq 10^5$ rad/sec. The error $\Delta\omega/\omega$ is thus $(10^5/2\pi\times 10^7)\simeq 0.2\%$.

With CW crystal oscillators the frequency determination is trivial and may be carried out with essentially unlimited accuracy.

*4. Check of "interference removers."* To determine the effectiveness of the "interference removers" the following checks were made: Both start and stop inputs were

[20] W. Weber, C. W. Johnstone, and L. Cranberg, Rev. Sci. Instr. 27, 166 (1956).

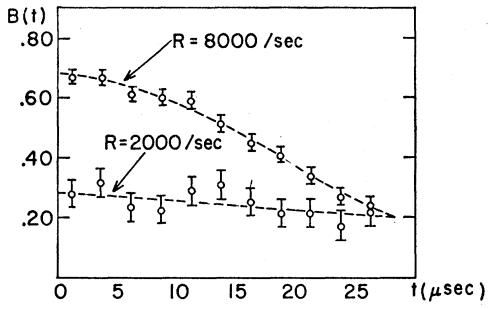


FIG. 4. Isolated "growth background," recorded at an instantaneous $\mu^+$ rate $R=1700$/sec. This background is due to multistop events as illustrated in Fig. 8, case (*c*).

driven from independent random sources with the "interference removers" switched off. The resulting distribution was of the expected form,

$$O(t)=e^{-t/\tau}, \quad \tau=(\text{stop rate})^{-1}. \tag{10}$$

The same sources were measured with the "removers" switched on, and the distribution

$$O(t)=\text{constant}$$

was found to an accuracy of 0.1% per channel.

### B. Background Investigations

In Sec. II-C two types of events leading to a time-dependent background level were described. It was pointed out that one of these, the "growth background," could be isolated electronically and suppressed during the actual lifetime measurements. It is also possible to select electronically *just* these events, suppressing all true decay events; this affords a valuable check of at least one critical part of the background theory, i.e., that which leads to expression (AI8) deduced in Appendix I. The results of such a "growth background" measurement are presented in Fig. 4. The agreement between theory and experiment is seen to be excellent.

A second time-dependent background effect (case I(d) of Appendix I) was studied by making runs at high muon rates in the "normal" order and displaying a large time range before $t=0$. The results of two such measurements are presented in Fig. 5. Again the observed effects are seen to be in good quantitative agreement with theory.

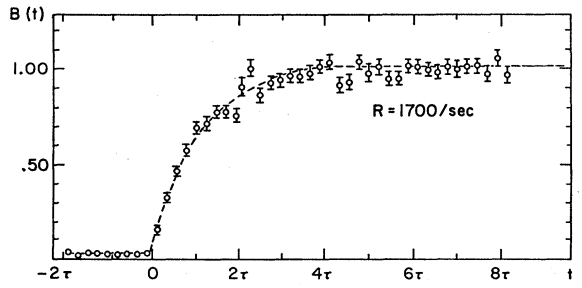


FIG. 5. Isolated background due to decays from $\mu^+$'s stopping during dead-time $T_d$ preceding current analysis; instantaneous $\mu^+$ rates given in figure. The time sequence involved in this type of event is illustrated as case (*d*) of Fig. 8.

### C. Data Runs

The relevant features and the results of twelve independent data runs are summarized in Table I. Runs 1 and 2 were made with an earlier version (predominantly vacuum tube) of digitron embodying a pulsed timing oscillator of about 10 Mc/sec.[9] An interference remover was employed on the stop pulse input only and the uncorrelated electron rate $f$ (not measured directly) was considerably greater than the value of 3% achieved in later runs (5 through 12). A stationary cyclotron target giving $D=50$ was used. These facts account for the relatively poor $\lambda$ of these runs.

Runs 3 and 4 were performed in the "inverted" order, using a vibrating target that gave $D\approx 4$, and with a digitron embodying a 5-Mc/sec CW crystal oscillator, and two interference removers. The uncorrelated $e^+$ rate was about as high as in runs 1 and 2.

In runs 5–12 the same digitron was used as in runs 3 and 4, but it was modified to 4 Mc/sec. Runs 5 through 9 were done in the "inverted" order, runs 10 through 12 in the normal order. In conjunction with each of these seven runs, $D$ and $f$ were measured; note that $R$ was varied by a factor 8 during this set of runs.

Knowing $\omega$, $D$, $f$, and $r$, relation (6) was used to calculate the expected background. This $B_{\text{calc}}$ must be compared with the value $B_{\text{fit}}$ found from the least-squares fit to the data at $t>0$ (see Sec. III-D), as well as with $B_{\text{exp}}$, the value found from the data recorded at $t<0$. The fractional solid angle $\omega$ (0.23 in practice) could easily be measured to the necessary accuracy from the $e^+$ and $\mu^+$ rates or else be calculated for the simple geometry involved. $D$ was determined from relation (8), and $f$ was measured by running digitron in the inverted order and recording the fraction of unstopped starts, i.e., the percentage of $e^+$'s that had no parent.

### D. Data Analysis

During the actual measurements, a preliminary value of $\tau(\mu^+)$ was extracted from the data by using $B_{\text{exp}}$ (when available) and analyzing the "net" time distribution by an appropriate slight modification (see Appendix II) of Peierls' method.[21] The values found in this way were in excellent agreement with those found by the method described below.

The final analysis consisted in making least-squares fits of the data to an expression of the form $N\exp[-t/\tau(\mu^+)]+B_0$, by means of an electronic computer.[22] The program gave the values of the three

[21] R. Peierls, Proc. Roy. Soc. (London) **A152**, 23 (1935).
[22] University of Chicago "Univac."

TABLE II. Recent measurements of $\tau(\mu^+)$.

| Source | $\tau(\mu^+)$, $\mu$sec | max | $\lambda$ | min | Method |
|---|---|---|---|---|---|
| Cern[a] | 2.20 ±0.015 | | 120 | | Scope trace photography |
| Carnegie Tech[b] | 2.211±0.003 | 450 | | 30 | Digital analyzer |
| Chicago[c] | 2.208±0.005 | 590 | | 330 | Digital analyzer |
| Liverpool[d] | 2.225±0.006 | | 1400 | | Time-to-pulse-height converter |
| This paper[e] | 2.203±0.004 | 23000 | | 330 | Digital analyzer |
| Weighted mean | 2.210±0.002 | | | | |

[a] See reference 7.
[b] See reference 8.
[c] See reference 9.
[d] See reference 10.
[e] This value includes the data of reference 9.

parameters $B_0$, $N$, $\tau(\mu^+)$, their variances $(\delta B_0)^2$, $(\delta N)^2$, $[\delta\tau(\mu^+)]^2$, and the $\chi^2$ of the fit.

An additional fit was made to the function

$$N\exp[-t/\tau(\mu^+)]+B_0+2N[t/\tau(\mu^+)]^2K \times\exp[-t/\tau(\mu^+)]; \quad (11)$$

the parameter $K$, the so-called "curvature" of the exponential function, is a measure of the "purity" of the exponential.

Values of $K\neq 0$ would indicate that the data would be better fitted by a sum of two exponential functions, and thus be of doubtful value for a determination of $\tau(\mu^+)$. In addition to computing the three parameters $B$, $N$, $\tau(\mu^+)$ and their variance, this program gave $K$, its variance $(\delta K)^2$, and $\chi^2$ for the fit.

### E. Summary of Results

A comparison of the values of $B_{\text{fit}}$, $B_{\text{calc}}$, and $B_{\text{exp}}$ given in Table I indicates good agreement between these three quantities. Blank entries in the columns corresponding to runs 1–4 are due to the fact that for these the values of $f$ were either unknown or else only inadequate data for $t<0$ were available. For runs 10–12, $B_{\text{exp}}$ is not listed, as we consider its value unreliable because of the effects mentioned in Sec. II-C.

We thus have reason to believe that *backgrounds* are quantitatively understood at least for the great majority of our runs, and hence should not be a serious source of systematic error.

The next source of such errors of which we are aware is the possible rate dependence of the measurements. Figure 6, drawn with the data of Table I, shows the distribution of $\tau(\mu^+)$ values vs $R$, the instantaneous muon stop rate. The dashed line indicates the weighted mean, $\langle\tau(\mu^+)\rangle$, of the entries. Inspection of Fig. 6 shows no obvious rate dependence.

The weighted mean value $\langle K\rangle$ for the 12 runs is $(-0.2\pm0.3)\times10^{-3}$. The distribution of individual values around the mean is shown in Fig. 7. Each value is zero within a reasonable error and this indicates that the data are well fitted by a single exponential function.

The goodness of the fits to the individual data runs is also substantiated by their $\chi^2$ values; $\langle\chi^2\rangle$ in Table I is the expected value.

The weighted mean of the twelve $\tau(\mu^+)$ values listed in Table I, i.e., our final result, is

$$\tau(\mu^+)=(2.203\pm0.004)\ \mu\text{sec}. \quad (12)$$

The errors in $\tau(\mu^+)$ given in Table I are mean standard deviation as found with the least-squares fit program. From these statistical errors of the individual values alone, an error of $\pm0.001$ $\mu$sec would have had to be attached to their mean. The distribution of the individual values about their mean (Fig. 6) is wider than expected ($\chi^2=19$ found vs $\chi^2=11\pm5$ expected) and doubling of the individual errors alone is required to bring the found and the expected $\chi^2$ values into agreement. We hence assign an error (to 98% confidence level) of 0.004 to $\tau(\mu^+)$ computed from the variance of the *observed* distribution.

## IV. CONCLUSIONS

The value $\tau(\mu^+)=(2.203\pm0.004)$ $\mu$sec found here is lower than all previously reported values of comparable

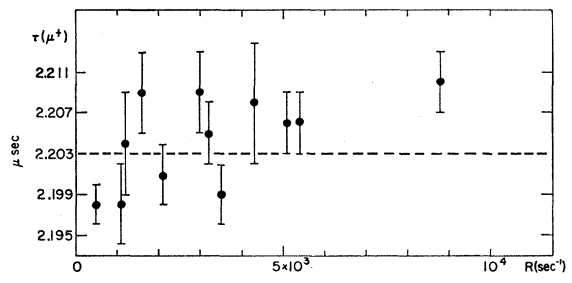


FIG. 6. Plot of $\tau(\mu^+)$ vs instantaneous $\mu^+$-rate $R$. Dashed line indicates weighted mean, $\langle\tau(\mu^+)\rangle$.

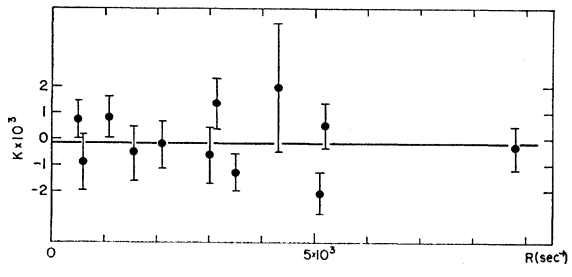


FIG. 7. Plot of "curvature" $K$ [as defined in Eq. (11)] vs instantaneous $\mu^+$-rate $R$. Dashed line indicates weighted mean, $\langle K\rangle$.

accuracy; these are compiled for convenience in Table II. Of these previous values, the one based on the most detailed experiments was that of Reiter *et al.*[8] who found $(2.211\pm0.003)$ $\mu$sec. Our value is significantly less than this. In view of the larger backgrounds and lack of precautions against instrumental distortions of the "interference" kind (see Sec. II-C), this disagreement may be due to systematic effects from these sources.

The disagreement between the current theoretical predictions and either our $\tau(\mu^+)$ or the mean of all recent determinations, $\tau(\mu^+)=(2.210\pm0.002)$ $\mu$sec, is quite large; in our opinion it is unlikely that it is due to experimental errors in the measurement of $\tau(\mu^+)$.


## ACKNOWLEDGMENTS

I would like to thank Professor V. L. Telegdi for proposing this experiment and for his encouragement and critical advice which contributed greatly to its progress. I wish to express my appreciation to J. Lathrop and R. Winston for their unfailing efforts in the preparation and performance of this experiment, as well as to R. Swanson and D. Yovanovitch for their assistance in its preliminary phases and for helpful discussions. The able technical assistance of D. Norman was much appreciated.


## APPENDIX I[23]

The digitron is a device designed to determine a differential interval distribution between pairs of events presented at its input, say $I(t)$. This input distribution is mapped into a differential output distribution of intervals, say $O(t)$. The central point that needs emphasis is the fact that $I(t)=O(t)$ when, and only when, a single "source" provides $I(t)$. The term "source" has here the meaning of a physical process which can provide but a single stop count for each start count. Muon decay and background electrons are two distinct "sources" in this sense. On the other hand, a negative muon in a chemical compound, capable of giving decay electrons with two distinct decay rates, is a single "source" within this definition, inasmuch as it can provide one and only one decay electron, i.e., stop pulse.

The digitron gives an output if, after a start pulse at $t=0$, no stop pulse occurs up to a time $t'=t$, and a stop pulse does occur between $t$ and $t+dt$. The probability of no stop occurring before $t=t'$ clearly equals the probability of a stop occurring for $t'>t$:

$$D(t)=\int_t^\infty I(t')dt', \quad \text{with} \quad D(0)=\int_0^\infty I(t')dt'=1. \quad \text{(AI1)}$$

Obviously,

$$I(t)=-dD(t)/dt. \quad \text{(AI2)}$$

[23] These Appendixes are due to R. Winston.

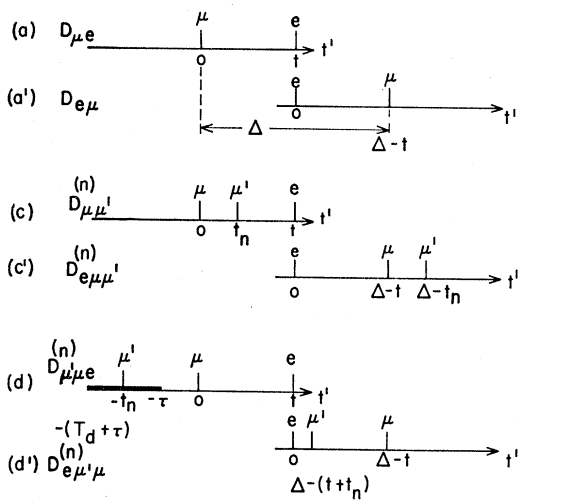


FIG. 8. Diagrams illustrating time sequences of various background sources as discussed in Appendix I.

The integral functions, say $D_i(t)$ in the case of several independent sources "$i$," have the advantage of following a simple law of composition, whereas the $I_i(t)$'s from which they are derived do not. The probability of not getting a stop count from several sources up to $t'=t$ is just

$$D(t)=\prod_i D_i(t), \quad \text{with} \quad D_i(t)\equiv\int_t^\infty I_i(t')dt'. \quad \text{(AI3)}$$

The output differential distribution $O(t)$ is hence given by

$$O(t)=-dD/dt=-(d/dt)\prod_i D_i(t)$$
$$=D(t)\sum_i[-(d/dt)\ln D_i(t)], \quad \text{(AI4)}$$

which gives $I(t)=O(t)$ in the case of a single source. The interference between the different sources is reflected in (AI4) through the factor $D(t)$.

By insuring that a given start pulse is followed, as far as recorded events are concerned, only by a single stop count within the measuring interval $T$, one effectively has the digitron sample alternately and independently the various "sources" $I_i(t)$ presented at its input. In this case, and in this case alone, the output $O(t)$ equals an incoherent superposition of the various $I_i(t)$'s. In practice, this condition can be achieved by means of the "interference removers" mentioned in the text (Sec. II-D-5). The general discussion given hereunder applies when no such "interference removers" are being used.

We shall now apply this general formalism to the time distribution of $e^+$'s from $\mu^+$ decay. For this purpose we shall analyze the input distribution, $I(t)$, into its independent components and derive the partial $D_i(t)$'s for each. For convenience, all times will be expressed in units of the $\mu^+$ lifetime.

The various combinations of stop and start pulses

which can lead to a recorded event in the digitron (i.e., the various "sources" referred to above) are illustrated in Fig. 8 for the "normal" and the "inverted" operations of the digitron, respectively. The subscripts to the various $D_i$'s are so chosen as to recall the nature of their "sources": $\mu$ for the muon of interest, $\mu'$ for another intervening muon, $e$ for a target (muon) originated $e^+$, $e'$ for an uncorrelated $e^+$.

### A. Natural Order

*One-Stop Events*

(*a*) *True decay events.* [See Fig. 8(a).]

$$D_{\mu e}=1-\omega(1-e^{-t}), \tag{AI5}$$

where $\omega$ is the fractional solid angle subtended by the $e^+$ telescope.

(*b*) *Events with parentless (uncorrelated) electrons* (not illustrated). A rate $B$ in the $e^+$ telescope, having no time correlation with muon stops, will give

$$D_{\mu e'}=e^{-Bt}. \tag{AI6}$$

*Multistop Events*

(*c*) *True decay events of uncertain parentage, additional muon(s) at $t'>0$.* [See Fig. 8(c).]

$D_{\mu\mu' e}\equiv\prod_n D_{\mu\mu' e}{}^{(n)}$, where, defining $R$ to be the muon stop rate,

$$D_{\mu\mu' e}{}^{(n)}\equiv D_{\mu\mu' e}(t_n)=1-\omega R(\delta t)_n(1-e^{-(t-t_n)}), \tag{AI7}$$

so that

$$D_{\mu\mu' e}=\exp[-\omega R(t+e^{-t}-1)]. \tag{AI8}$$

This covers the case of an arbitrary number of muons stopping, at times indicated as $t_n$ in the interval 0 to $t$.

(*d*) *True decay events of uncertain parentage, additional muons at $t'<0$.*[24] Muons in this category must of necessity stop within the dead time $T_d$ of a previous analysis. [See Fig. 8(d).]

For a given time $\tau$ separating the end of a previous analysis from $t=0$, one has

$$D_{\mu'\mu e}(\tau)=\prod_n D_{\mu'\mu e}{}^{(n)}(\tau),$$

where

$$D_{\mu'\mu e}(\tau)=1-\omega R(\delta t)_n e^{t_n}(1-e^{-t}), \qquad -(T_d+\tau)<t_n<-\tau, \tag{AI9}$$

so that, since $e^{-T_d}\approx 0$, ($T_d\approx 200$ for the digitron used here), one obtains

$$D_{\mu'\mu e}(\tau)=\exp[-\omega R(1-e^{-t})e^{-\tau}]. \tag{AI10}$$

Finally, $D_{\mu'\mu e}(\tau)$ must be averaged over the Poisson-distributed $\tau$'s, yielding

$$\bar{D}_{\mu'\mu e}=\int_0^\infty D_{\mu'\mu e}(\tau)Re^{-R}d\tau \simeq 1-R^2(1-e^{-t})+\text{order}(R^3). \tag{AI11}$$

[24] The treatment in this subsection is mostly due to R. A. Swanson to whom we are indebted for advice.

With the aid of Eq. (AI4), the composite $O(t)$ directly follows. Since $R$ and $B$ are small in practice ($<0.02$), the above exact expressions may first be simplified by linearizing in $R$ and $B$. The final result is

$$O(t)=\omega e^{-t}\{1-\omega R[t+2(e^{-t}-1)+(1-\omega)/\omega]-B(t-1)\} +(1-\omega)(\omega R+B). \tag{AI12}$$

One sees that the background is neither flat nor simply sloped but has the appearance of a growth curve, starting from $B$ at $t=0$ and increasing to its maximum value, $(1-\omega)(\omega R+B)$, with a "lifetime" nearly that of the muon.

### B. Inverted Order

The muon pulse is delayed at the input by $\Delta\gg 1$ ($\Delta\simeq 10$ in practice). We shall characterize the sources of counts according to the sequence of events in the natural order.

*One-Stop Events*

(*a'*) *True decay events.* [See Fig. 8(a').]

$$\begin{aligned} D_{e\mu}&=1-e^{-(\Delta-t)}, \quad 0\leq t\leq\Delta,\\ &=0, \quad t>\Delta. \end{aligned} \tag{AI13}$$

(*b'*) *Events with parentless electrons* (not illustrated).

$$\begin{aligned} D_{e'\mu}&=D_{e\mu'\mu}, \quad 0\leq t\leq\Delta,\\ &=D_{e\mu'\mu}(\Delta)e^{-Rt}, \quad t>\Delta, \end{aligned} \tag{AI14}$$

where $D_{e\mu'\mu}$ is given below.

*Multistop Events*

(*c'*) *True decay events of uncertain parentage, additional muon(s) following $\mu$.* [See Fig. 8(c').]

$$D_{e\mu\mu'}=1. \tag{AI15}$$

(*d'*) *True decay events of uncertain parentage, additional muon(s) preceding $\mu$.* [See Fig. 8(d').]

$$D_{e\mu'\mu}=\prod_n D_{e\mu'\mu}{}^{(n)},$$

where

$$D_{e\mu'\mu}{}^{(n)}=1-R(\delta t)_n[1-\omega(1-e^{-(\Delta-t_n)})], 0\leq t\leq\Delta,$$

so that, since $e^{-\Delta}\approx 0$,

$$D_{e\mu'\mu}=\exp\{-R[(1-\omega)t+\omega e^{-(\Delta-t)}]\}, \quad 0\leq t\leq\Delta. \tag{AI16}$$

Since true events occur with relative frequency $R/(\omega R+B)$, while parentless events occur with relative frequency $B/(\omega R+B)$, we have the final distribution

linearized in $R$,

$$O(t)=[\omega R/(\omega R+B)][e^{-(\Delta-t)}\{1-R[(1-\omega)(1+t)+2\omega e^{-(\Delta-t)}]\}+R(1-\omega)+\omega e^{-(\Delta-t)}]$$
$$+[B/(\omega R+B)]R[(1-\omega)+\omega e^{-(\Delta-t)}],\quad 0\leqslant t\leqslant\Delta;\quad O(t)=B/(\omega R+B),\quad t>\Delta. \quad \text{(AI17)}$$

We have omitted from consideration the $e\mu'\mu$ events for which $\mu'$ occurs within the dead-time of a previous analysis, since such events contribute only terms of order $R^2$ to the total distribution.

## APPENDIX II

In applying Peierls' method for determining lifetime,[21] one needs to know the mean time $\bar{t}_n$ of events in the $n$th channel. Due to the finite channel width $d$, $\bar{t}_n \neq t_n$, the channel midpoint, but one has instead,

$$t_n-\bar{t}_n=\int_{-\infty}^{\infty} sp_n(s)ds \Big/ \int_{-\infty}^{\infty} p_n(s)ds,\quad s\equiv t-t_n, \quad \text{(AII1)}$$

where $p_n(s)$ is the relative probability for an event to occur at time $t$ and be stored in the $n$th channel. $p_n(s)$ is clearly the product of $O(t)$, the output time distribution of events, and $R_n(s)$, the channel resolution. $R_n(s)$ is the probability for an interval of length $t$ to be sorted into the $n$th channel. Therefore,

$$\bar{t}_n-t_n=\int_{-\infty}^{\infty} sO(s+t_n)R_n(s)ds \Big/ \int_{-\infty}^{\infty} O(s+t_n)R_n(s)ds. \quad \text{(AII2)}$$

$R_n(s)$ can be determined empirically by means of pairs of "delta" pulses of varying separation. For the digitron used here it has, both in theory and in practice, the triangular form (independent of $n$)

$$\begin{aligned} R(s)&=(d+s)/d^2, && -d\leqslant s\leqslant 0,\\ &=(d-s)/d^2, && 0\leqslant s\leqslant d,\\ &=0, && \text{otherwise.}\end{aligned} \quad \text{(AII3)}$$

In the absence of background, (or subtracting it before analysis), $O(t)=e^{-t}$. Using Eq. (AII2), this gives

$$\bar{t}_n-t_n=d^2/6+\text{order}(d^4). \quad \text{(AII4)}$$

Peierls assumes that $R(s)$ has the "box-like" form

$$\begin{aligned} R(s)&=1/d, && -d/2\leqslant s\leqslant d/2,\\ &=0, && \text{otherwise,}\end{aligned} \quad \text{(AII5)}$$

which gives

$$\bar{t}_n-t_n=d^2/12. \quad \text{(AII6)}$$

For most of our measurements, $d\simeq 0.1$, so that it was important to use the pertinent expression, i.e., (AII6) rather than (AII4).

PHYSICAL REVIEW VOLUME 125, NUMBER 5 MARCH 1, 1962

# Measurement of Total Cross Sections of $K^-$ Mesons in Hydrogen and Deuterium in the Momentum Region 630 to 1100 Mev/$c$*

O. CHAMBERLAIN, K. M. CROWE, D. KEEFE, L. T. KERTH, A. LEMONICK,† TIN MAUNG, AND T. F. ZIPF
*Lawrence Radiation Laboratory, University of California, Berkeley, California*

(Received October 16, 1961)

Total cross sections of $K^-$ mesons in hydrogen and deuterium were measured over the momentum range 630 to 1100 Mev/$c$. The $K^-$—$n$ total cross sections were obtained from deuterium and hydrogen data. A well-defined resonance appeared in the $K^-$—$p$ total cross section at about 1000 Mev/$c$. Two high-resolution velocity-selecting Čerenkov counters were used to select $K^-$ mesons. The momentum resolution was within 1% to 2%, and the momentum intervals chosen were very closely spaced.

## I. INTRODUCTION

In a recent experiment Cook *et al.*[1] have made an extensive study of the behavior of the $K^-$-meson cross sections on protons ($\sigma_p$) and neutrons ($\sigma_n$) in the momentum region 1 to 4 Bev/$c$. They have shown the existence of structure in $\sigma_p$ and, in particular, evidence for variations in the behavior of the isotopic spin components $I=1$ and $I=0$. At low energies, measurements of total cross sections from emulsion and bubble chamber work[2] show that for momenta below a few

* Work done under the auspices of the U. S. Atomic Energy Commission.

† Present address: Palmer Physical Laboratory, Princeton University, Princeton, New Jersey.

[1] V. Cook, B. Cork, T. F. Hoang, D. Keefe, L. T. Kerth, W. A. Wenzel, and T. F. Zipf, Phys. Rev. **123**, 320 (1961).

[2] L. W. Alvarez, *Ninth International Conference on High-Energy Physics, Kiev, 1959* (Academy of Sciences, Moscow, 1960), Plenary Session I–V, p. 471. See also L. W. Alvarez, University of California, Lawrence Radiation Report UCRL-9354, 1960 (unpublished).